MEDDOCS Open Access Publisher

Annals of Forensic Science and Research

Open Access | Research Article

Covid-19 Identification Using Graphene Oxide and Gold Nanoparticles

Maryam Davardoostmanesh[1]; Hossein Ahmadzadeh[1]*; Ida Attari Navab[1]; Elham Zaeif Khorasani[2]; Maryam Ijadi Bajestani [1]

[1]Department of Chemistry, Faculty of Science, Ferdowsi University of Mashhad, Mashhad 9177948974, Iran.

[2]Internal Medicine, Medical University of Mashhad, Mashhad 9177899191, Iran.

***Corresponding Author(s): Hossein Ahmadzadeh**

Department of Chemistry, Faculty of Science, Ferdowsi University of Mashhad, Mashhad 9177948974, Iran.

Email: h.ahmadzadeh@um.ac.ir

Received: Apr 17, 2023

Accepted: May 11, 2023

Published Online: May 18, 2023

Journal: Annals of Forensic Science and Research

Publisher: MedDocs Publishers LLC

Online edition: http://meddocsonline.org/

Keywords: Covid-19 N-protein; Point of care; Lateral flow immunoassays; Spherical gold nanoparticles; Graphene oxide nanosheets

Abstract

Fully dispersible spherical gold nanoparticles (AuNPs) and stable graphene oxide nanosheets (GO) were prepared, characterized and used as nano-labeling for the Lateral Flow Immunoassays (LFIA) based Point-of-Care (POC) monitoring of Covid-19 nucleocapsid (N) protein in clinical samples. The Covid-19 N-protein was immobilized onto the test line of the strip, and IgG protein was conjugated with nanolabels to form the detectable intensity. The results are achieved within 15 min. The effect of different sizes and concentrations of nanolabels in test line intensity were also evaluated. As-prepared LFIA based AuNPs and GO labels revealed visual LOD of 3.0 and 0.1 mg mL^{-1} for Covid-19 N-protein, respectively. The LFIA test was performed on ten positive and negative serum samples including patients, healthy and carrier people to demonstrate the clinical feasibility of our proposed assay for Covid-19 identification. This work presented a simple, low cost, and fast method for the diagnosis of Covid-19 in the clinical samples.

Article Highlights

- The lateral flow immunoassays detect analytes through color-forming reaction on a membrane based on label accumulation.
- Gold nanoparticles and graphene oxide nanosheeets as labels provide a high visual intensity on LFIA membranes.
- The signal intensity correlates with the size and concentration of the nanolabels.

Introduction

In December 2019, the emergence of coronavirus disease (Covid-19) was reported in Wuhan city of China, which quickly became a pandemic global public health concern as declared by the World Health Organization (WHO)[1]. This virus spread quickly and led to serious respiratory diseases pandemic and paralyzed the world. Since some patients who infected with Covid-19 are asymptomatic, an early and precise diagnosis of suspected cases is essential to control the epidemy. Some commonly used methods, including real-time Reverse Transcription-Polymerase Chain Reaction (RT-PCR) and RNA sequencing are known as standard methods with high accuracy for laboratory diagnosis of Covid-19 [2-4]. However, these methods require long detection times, experienced operators, and complex equipment, which limit their applications for Point-Of-Care Testing (POC) diagnosis. Thus, the development of a rapid detection method is crucial to facilitate on-site diagnosis of Covid-19. In

Cite this article: Maryam D, Hossein A, Ida A, Elham ZK, Maryam I. Covid-19 Identification Using Graphene Oxide and Gold Nanoparticles. Ann Forensic Sci Res. 2023; 2(1): 1007.

this way, Lateral Flow Immunoassay Test (LFIA) as a POC technology can be a suitable choice for the effective screening due to its low cost, simplicity, rapidity and portability which is able to accurately distinguish Covid-19 from other respiratory viral infections [5-8]. It can detect analytes through color-forming reaction on a paper membrane based on label accumulation [9]. Wen et al.[10] used LFIA test for the detection of severe acute respiratory syndrome coronavirus 2 (SARS-CoV-2). The LFIA test was performed by labeling of anti-human IgG with gold nanoparticles (AuNPs) and immobilizing SARS-CoV-2 nucleocapsid protein on the surface of the strip. In the last few years, various fluorescent labels such as quantum dots and upconversion, and lanthanide complexes have been used as labels in LFIA technology [11-14]. Although fluorescent labels provide high sensitivity, additional apparatus for visual detection, limit the simplicity of LFIA tests. In contrast with other reporting labels, AuNPs and graphene derivatives are commonly used labels in lateral flow tests due to their excellent biocompatibility [15,16]. AuNPs can easily be conjugated with biomolecules via adsorption process and create visible signal because of their surface plasmon properties [17]. Graphene derivatives especially graphene oxide (GO) with a large variety of oxygen-containing functional groups having great potential for labelling biomolecules provide a high visual intensity on LFIA membranes [18]. These features enhance the application of disposable and inexpensive LFIA test strips with high sensitivity. There are several reports on the use of AuNPs and graphene derivatives as labels in a LFIA system [19-21]. Yu et al.[21] used GO and carboxylated GO as labels for fast detection of aflatoxin B1 using LFIA test. They concluded that compared with GO, the carboxylated GO with more oxygen containing functional groups can easily migrate through the membrane pores when used as a label. This work compares the potential of AuNPs and GO as labels for the detection of Covid-19 using LFIA technology. Because the optical response of labels is size and concentration dependent, several parameters such as size and concentration of nanomaterials were also optimized. By choosing the optimal conditions, this method was also applied to real sample for Covid-19 screening.

Materials and methods

Chemicals

Nitrocellulose membrane (NC) (VIV902503R) from PAL (USA), anti-mouse IgG and nucleocapsid N-protein of Covid-19 from Bu Ali Research Institute (Mashhad, Iran), graphite powder (<0.1 mm, >95 %) from Fluka, cetyltrimethylammonium bromide (CTAB) (98%) from ALFIA Aesar, trisodium citrate (97%) from GPR, potassium permanganate (99%) from BDH, hydrogen peroxide (30%) from Fakhre Razi, sodium nitrate (99%), sulfuric acid (95%), hydrogen chloride (37%), barium chloride (99%), silver nitrate (99.5%), ascorbic acid (99.5%), and sodium borohydride (96%) were purchased from Merck and used with no further purification. All aqueous solutions were prepared with deionized (DI) water.

Instruments

The UV-vis absorption spectra were measured by Photonix Ar 2015 UV-vis spectrophotometer. The atomic force microscopy (AFM) images of the samples were obtained from 0101/A AraResearch in a non-contact mode at room temperature. The transmission electron microscopy (TEM) images of the samples were recorded using a CM120 TEM at 120 kV. The color intensity was digitized using Image J software.

Preparation of nanomaterials

Preparation of $HAuCl_4$-$3H_2O$: The procedure is reported elsewhere [22]. Briefly, 10 mL of aqua regia (75% v/v HCl, 25% v/v HNO_3) was slowly added to about 0.1 g of small pieces of metallic gold. The mixture was stirred and gradually heated until the temperature was increased to 70 °C and the metallic gold was completely dissolved. The composed brown nitric vapors were eliminated by slowly adding HCl to the solution. This procedure was repeated about 5 times, until, no brown nitric vapor was evolved with addition of HCl. In order to complete the removal of acid vapors, doubly distilled de-ionized water was added to the solution under stirring until the solution was concentrated. This operation was repeated twice. A litmus paper was used to check the presence of acid vapors, until pH 7 was reached. The solution was heated at 70 °C to concentrate it to about 4 mL and then the solution was cooled to room temperature. The beaker was placed into a desiccator under vacuum including a dish containing concentrated H_2SO_4. After about two weeks, yellow color crystals were formed.

Preparation of gold seeds: Firstly, 10 mL aqueous solution of 0.5 mM trisodium citrate was added to 10 mL aqueous solution of 0.5 mM $HAuCl_4$. Then, 0.6 mL of freshly prepared 0.1 M $NaBH_4$ solution (ice-cold) was slowly added to the solution while stirring. The solution was stirred 2 h and the particles produced in this solution were used as seeds for the growth of gold nanoparticles [23].

Preparation of growth solution: Solid CTAB (3 g) was added to the 200 mL of $HAuCl_4$ (0.5 mM) and it was heated up to about 50 ^{O}C until the solution became clear. The solution was used as a stock growth solution [23].

Different size preparation: In the next stage, 2 mL of seed solution was mixed with 18 mL of growth solution and 0.1 mL of freshly prepared 0.1 M ascorbic acid solution while stirring. Similarly, 2 mL of seed solution was mixed with 10 and 5 mL of growth solution and 0.1 mL of 0.1 M ascorbic acid solution, respectively. Particles were prepared in each stage with different sizes. Finally, the resulting nanoparticles were centrifuged thrice at 6000 rpm for 15 min, and washed with deionized water several times.

Preparation of GO: GO was synthesized using modified Hummers' method [24]. Briefly, graphite powder (2 g) was gradually added to 70 mL concentrated H_2SO_4 in an ice bath. Then, 24 mmol $NaNO_3$ and then 38 mmol potassium permanganate was gradually poured into the mixture while stirring with temperature control. After that, the suspension stirred at room temperature for 48 h. Subsequently, 100 mL DI water was added to the mixture followed by further dilution by warm water (35 °C). Then, 70 mL H_2O_2 was added within 30 min. The product was centrifuged and washed several times with HCl (5 wt %) and then with DI water. The effluent was tested using BaCl2 and AgNO3 to ensure the complete removal of SO_4^{2-} and Cl^- ions, respectively. The final product was freeze dried at -48 °C for 2 days.

Size separation of GO sheets: The process of size separation of GO sheets is depicted in Scheme 1. Proper amount of GO was dispersed in deionized water and centrifuged at 2000 rpm for 10 min. The resultant mixture was separated into the supernatant and precipitated by decantation. The precipitate was dried and named as GO1. The supernatant was again divided into the supernatant and precipitate by repeating the centrifugation

step. The supernatant was dried and named as GO2. Bulk GO was named as GO0.

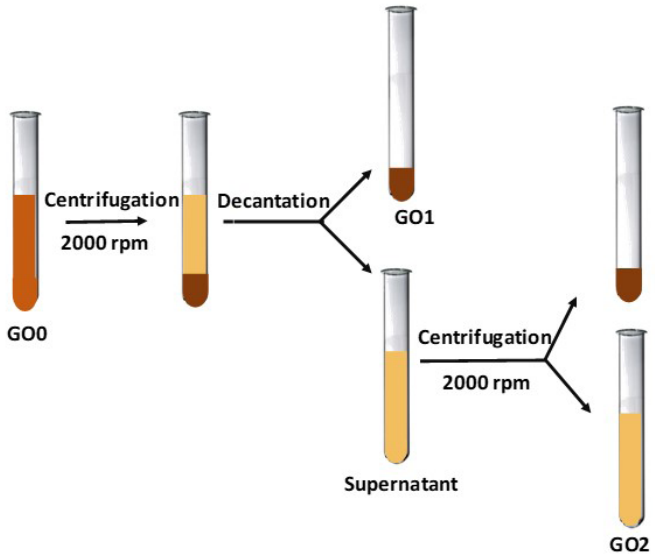

Scheme 1: Size separation of GO sheets using centrifugation.

Labeling of IgG protein with AuNPs and GO

Initially, sufficient amount of AuNPs was sonicated in phosphate buffer (2.5 mM, pH=8.8). Then, IgG (1 mg mL^{-1}) was added to AuNPs in various concentrations (1.0, 3.0, 6.0, 12.0, 24 mg mL^{-1}) and the resulting mixture was gently shaken for 30 minutes. Subsequently, the mixture was centrifuged at 10000 rpm for 10 min to remove the excess protein. The above procedure was used for the conjugation of various concentration of GO nanosheets (0.05, 0.1, 0.5, 1.0, 1.5 mg mL^{-1}) to 1 mg mL^{-1} IgG as well. Conjugate formation was confirmed by flowing the conjugates through NC membrane (2 cm length) that had been previously coated with Covid-19 N-protein in test zones. The accumulation of red and brown colors at the location of the test zone confirms functionalization of Au and GO with IgG, respectively. It should be noted that Covid-19 N-protein has fewer mutations than spike proteins. Therefore, this protein has been used in this study.

Preparation of immunochromatographic test strips

The prepared NC membrane was dried for 2 h and then, it was vertically immersed into sample mixture. Due to capillary action, the mixture moved along the pores of NC membrane, and the result was obtained within 15 min.

Analysis of clinical samples

Covid-19 N-protein with concentration of 5 mg mL^{-1} was deposited on the test zone on NC membrane surface. Then, the membrane was immersed into IgG protein solutions labeled with gold or GO nanomaterials for 10-15 min. After the completion of reaction in 15 min, the colorimetric signal on the test line (T line) was observed. The LFIA detection was performed on ten serum sample of healthy and infected individuals (triplicate experiments), and the visible data were collected and analyzed.

Result & Discussion

Characterization

UV-vis absorption spectra of Au-labeled antibody are shown in **Figure 1a**. The maximum absorption peak of AuNPs was centered at 521 nm, assigned to gold plasmon resonance band, indicating the formation of gold nanoparticles [20]. When the antibodies were bound to AuNPs, the absorption peak was red shifted to around 530 nm on the resulting Au-labeled antibody. Similar results were also observed for GO-labeled antibody **(Figure 1b)**. The GO sheets have an absorption peak at 230 nm assigned to the π-plasmon absorption of the C=C bond. Also, a weak shoulder at 300 nm is related to the n– π * transition of C=O [25]. IgG shows absorption peak at around 280 nm. When IgG labeled with GO, the weak shoulder at around 300 nm became sharper with a slight blue shift, indicating successful binding of IgG to GO sheets.

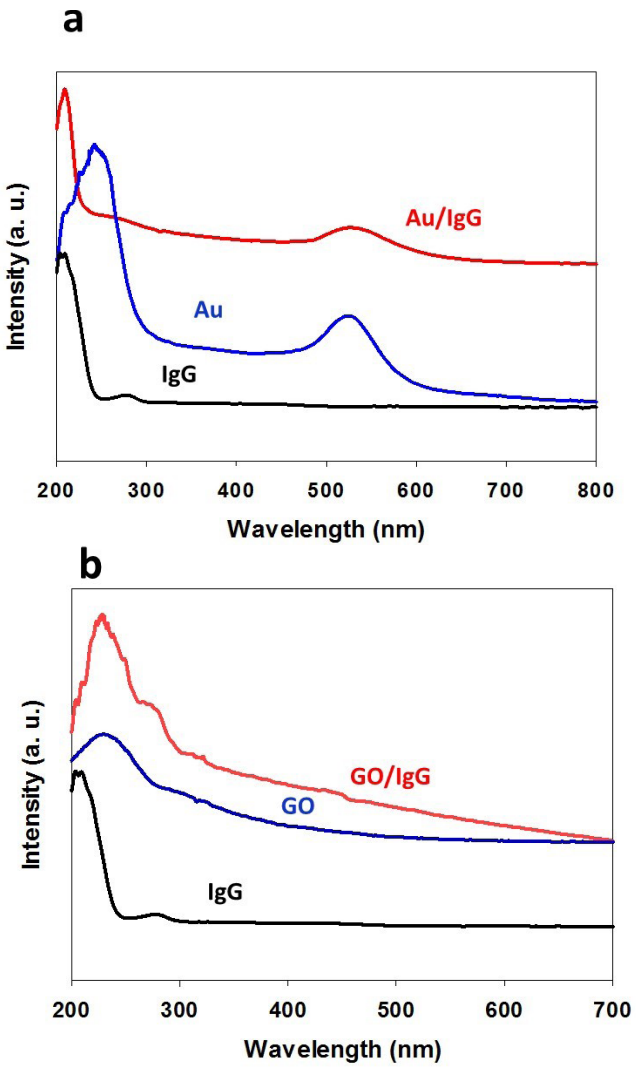

Figure 1: UV-vis absorption spectra of (a) Au, IgG, and Au/IgG; (b) GO, IgG, and GO/IgG. of **(a)** Au, IgG, and Au/IgG; **(b)** GO, IgG, and GO/IgG.

As shown in **Figure 2a-c**, the TEM image showed that the size of the synthesized AuNPs were 14, 19, and 30 nm in diameters. AFM images of GO sheets showed that the lateral dimensions of various sizes of GO sheets were 290 (GO2), 660 (GO1), and 560 (GO0) nm **(Figure 3a-c)**. The sheet size distribution was obtained by SPIP software [26].

The Au and GO labeled IgG were further characterized by TEM to confirm success of the labeling process.

Figure 4a shows the TEM image of AuNPs before conjugation with antibody. The observation of cluster-like structure after conjugation of AuNPs with antibody is clearly apparent **(Figure 4b)**. Presence of many wrinkles in TEM images of GO, suggest that the GO sheets are quite thin **(Figure 4c)**. Existence of bright spots on the surface of the GO confirms conjugation of GO sheets with IgG **(Figure 4d)**.

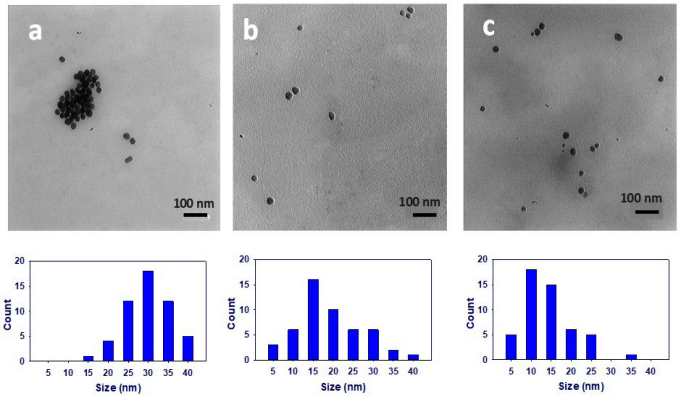

Figure 2: TEM images of different sizes of AuNPs **(a)** 30 nm; **(b)** 19 nm; **(c)**14 nm. The lower parts show the size distributions corresponding to each TEM image on the top.

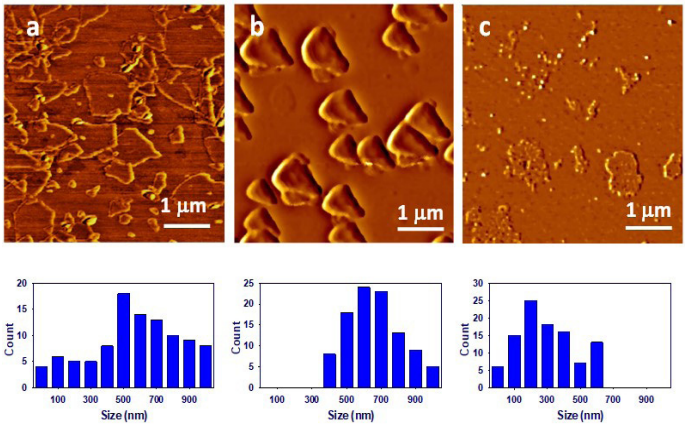

Figure 3: AFM images of different sizes of GO sheets **(a)** GO0; **(b)** GO1; **(C)** GO2. The lower parts show the size distributions corresponding to each AFM image on the top.

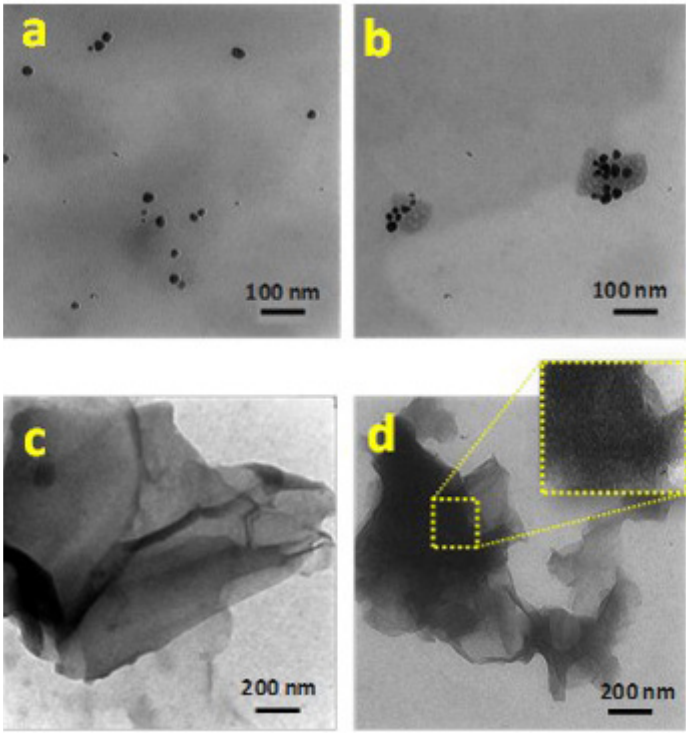

Figure 4: TEM images of the AuNPs **(a)** before and **(b)** after labeling with antibody; GO sheets **(c)** before and **(d)** after labeling with antibody.

Immunochromatographic assay

Scheme 2 shows the basic principle of the LFIA technique for the detection of Covid-19 in human serum samples based on typical antibody-antigen reactions as a competitive assay. In this assay, N- protein deposited on the T line of the NC membrane acts as the antigen. In case of viral infection, in response to the N-protein of the virus, body produces antibody (IgG and IgM). In the absence of the Covid-19 infection, the labeled IgG will bind to N- protein on the T line and forms the antigen-antibody complex. When there is an infection, there would be a competition between N-protein in the serum and N-protein on the T line for the labeled IgG, and therefore no visual spot on the T line. In this work, IgG protein (antibody) was labeled with AuNPs and GO nanosheets, which can bind to Covid-19 N-protein, specifically. T line was built on the LFIA test strip using Covid-19 N-protein (antigen). The sample solution migrates along the strip under capillary forces. Labeled IgG were captured by the N-protein of Covid-19 on T line to form immunocomplexes.

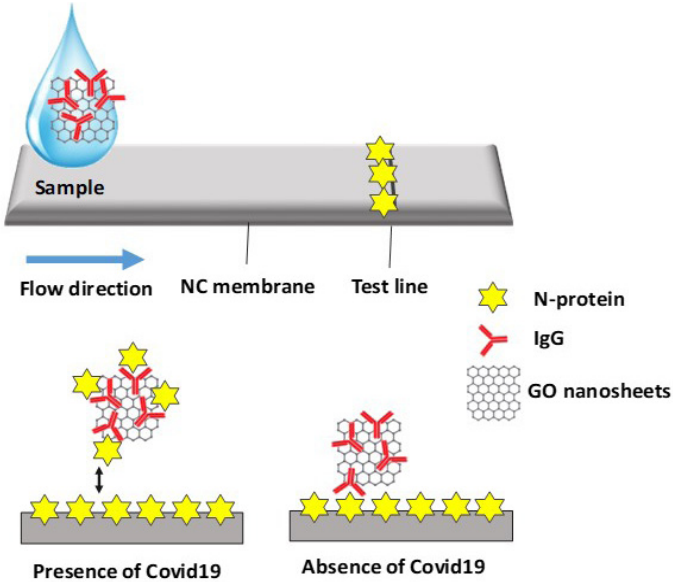

Scheme 2: Schematic of the LFIA test strip for detection of Covid-19.

Optimization of LFIA was carried out by altering the sizes and concentrations of nanomaterials and measuring the signal intensities on the corresponding T lines. IgG was conjugated with different sizes and concentrations of nanomaterials, and the color intensities on T line was measured and analyzed using Image J software.

The typical LFIA test strips using AuNPs with different concentrations and sizes conjugated with IgG are shown in **Figure 5a1 and 5a2**, respectively. The intense red color of AuNPs was appeared on T line resulting from the surface plasmon resonance at the nano-dimensional scale of AuNPs, typically from 10 to 60 nm. A high concentration of AuNPs resulted in an increase in the signal intensity of the T line **(Figure 5a1 and Figure 6a)**. With increasing the average AuNPs sizes from 14 to 30 nm, the signal intensity was also increased **(Figure 5a2 and Figure 6b)**. Several reports showed that the optimum size of about 30 nm AuNPs are suitable for conjugating proteins [20]. Zhang et al.[27] synthesized different sizes of AuNPs (33–195 nm) as LFIA labels. They concluded that the medium-size AuNPs (47-79 nm) were the most sensitive. There is an important correlation between the conjugate quality and size of the lable. Because of small cross sections of smaller particles, the density of antibodies conjugated with the labels can be reduced in order to lower

the intensity on T line. The optimal size and concentration of AuNPs was chosen to be 30 nm and 24 mg mL^{-1}. The LOD was defined as the minimum concentration of label that generates a detectable intensity on the T line. The lowest concentration of the AuNPs reliably detected at T line was 3 mg mL^{-1}. Therefore, the LOD of the strip test using AuNPs as label was 3 mg mL^{-1}.

The same experiments were performed for different concentrations and sizes of GO nanosheets conjugated with IgG (Fig. 5b1 and 5b2). The generated signal intensity correlates with the size and concentration of GO nanosheets **(Figure 6)**. The intense black color of GO provides a good contrast for visual detection. With increasing concentration of GO sheets, a more intense color was appeared on the T line **(Figure 5b1 and Figure 6a)**. Due to high aggregation of GO sheets in concentration above 1 mg mL^{-1}, no line appeared on T line. Also, small sheets showed higher intensity on test line **(Figure 5b2 and Figure 6b)**. Small GO sheets contain more oxygen containing functional groups. As a result, small GO-labeled IgG can easily migrate through the membrane pores, resulting a clear, visible line on the test zone. Therefore, in order to obtain the required visual observation of the results, the optimum size and concentration of GO sheets was set to be 290 nm and 1 mg mL^{-1}, respectively. The lowest concentration of the GO that can be reliably detected at T line was 0.1 mg mL^{-1}. Therefore, the LOD of the strip test using GO as label was 0.1 mg mL^{-1}.

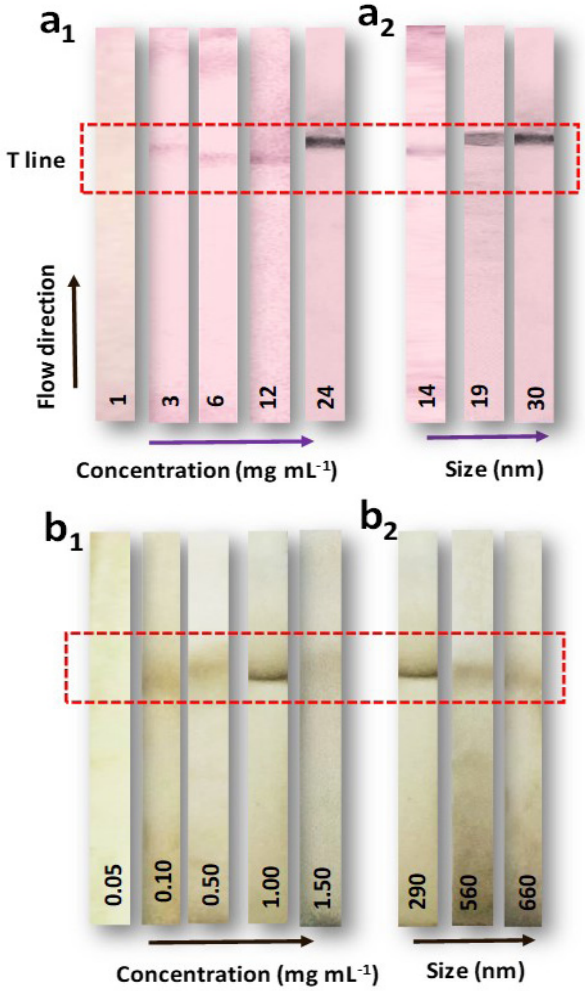

Figure 5: The typical LFIA test strip using **(a1)** Au-based label in different concentration (fixe size of 30 nm); **(a2)** Au-based label in different sizes (fixe concentration of 24 mg mL^{-1}); **(b1)** GO-based label in different concentration (fixe size of 290 nm); **(b2)** GO-based label in different sizes (fixe concentration of 1 mg mL^{-1}).

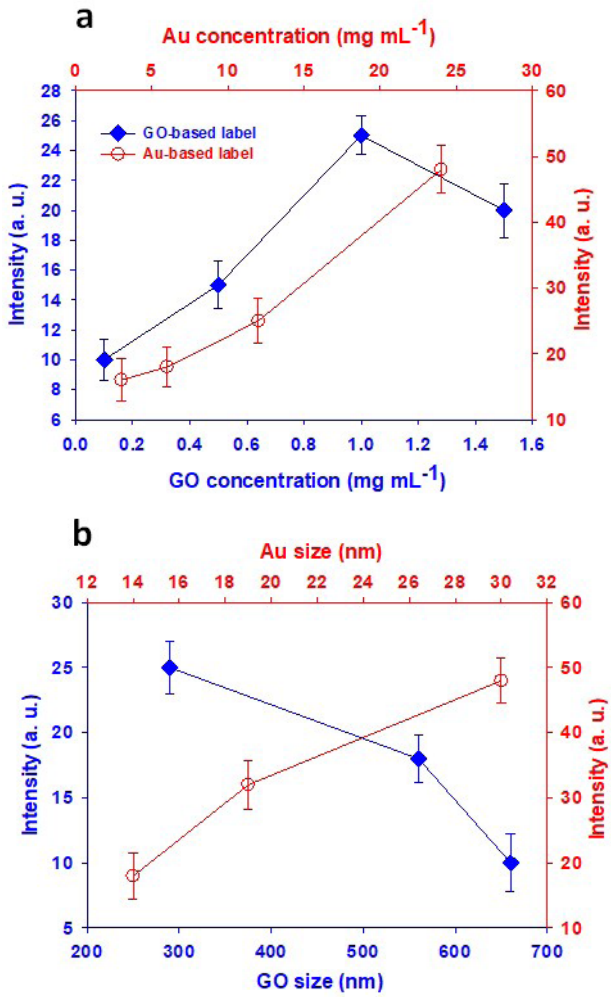

Figure 6: Color intensity on the test lines using Au-based label (top axis) and GO-based label (down axis) in different **(a)** concentrations and **(b)** sizes.

Detection of Covid-19 in real samples

The performance of LFIA was evaluated by testing serum samples obtained from Covid-19 patients and healthy people (confirmed by RT-PCR). Five clinical serum samples from patients with Covid-19 infected and five serum samples from healthy and carrier (vaccinated) people were collected. Fig.7 shows the detection results of the samples. The Covid-19 N-protein was immobilized on the T lines, while IgM and IgG were conjugated with nanomaterials to achieve sensitive detection of Covid-19 N-protein in serum samples. As shown in **Figure 7**, in this competitive immunoassay strategy, the color intensity of the T line was inversely related to the Covid-19 N-protein concentration in the sample. Most of healthy people's sera displayed a distinct signal at T line, while infected people showed no visible lines. However, the color intensity of the T line was not as sharp as for the carrier people's sera. Because Covid-19 N-protein is fixed on the T line, it can bind with antibody conjugated to the Au or GO nanomaterials. In the absence of Covid-19 N-protein in the healthy people's sera, labeled- antibody will bind with the Covid-19 N-protein on T line resulting in an intensive colored band on the T line **(Figure 6a)**. If the sample contains Covid-19 N-protein from the infection, the concentration of N-protein in the sample grows to be high, so that almost all conjugated antibodies will be occupied, and the labeled antibodies can freely pass the T line without any visible band on the test zone **(Figure 7b)**. For the carrier people's sera with low concentration of Covid-19 N-protein, the labeled- antibody will first react with

N-proteins in the serum, and the rest of conjugates would then be captured by the Covid-19 N-protein on the T line, resulting in the weak colored band at T line **(Figure 7a)**.

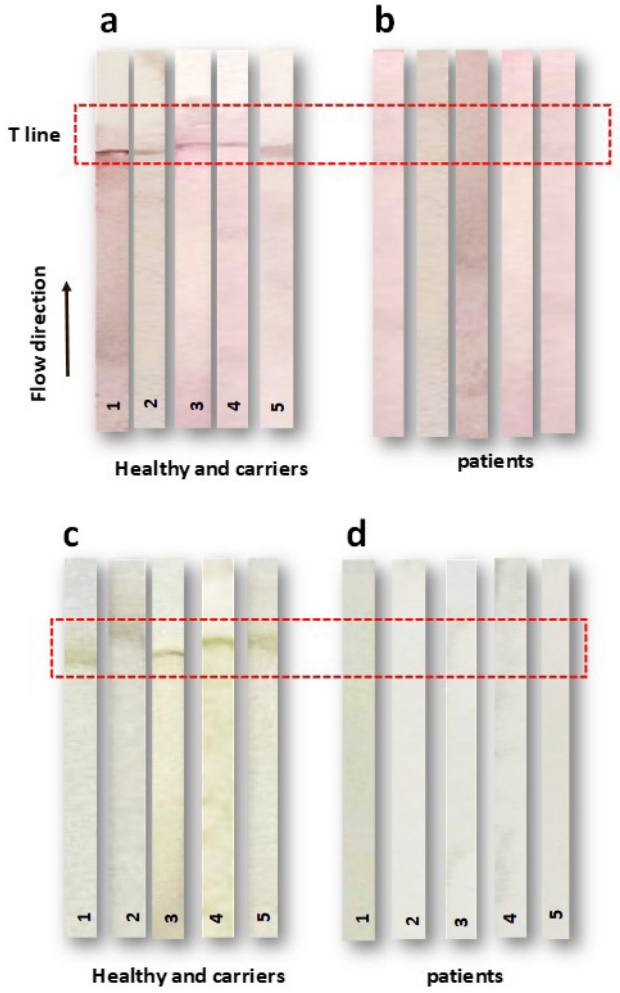

Figure 7: Detection of Covid-19 N-protein in real samples by LFIA test strip using **(a, b)** Au-based label; **(c, d)** GO-based label.

Conclusion

This work evaluated the possibilities of Au and GO as labels for IgG to detect the Covid-19 N-protein using LFIA technique. The results showed that the proper sizes and concentrations of nanolabels resulted in higher intensity or the color formation on test line. The LOD values for GO as a label was estimated to be 0.1 mg mL^{-1} which is 30 times lower than that of the Au as labels (3 mg mL^{-1}). The results were achieved within only 15 min. Considering several advantages of LFIA such as simplicity, low cost, and speed, it is a feasible method for the diagnosis of Covid-19 in urgent conditions.

Statements and Declarations

Declaration of competing interest

The authors declare that they have no competing financial interests or personal relationships that could have appeared to influence the work reported in this paper.

Data Availability Statement

The datasets generated during the current study are available from the corresponding author on reasonable request.

Author contribution

Maryam Davardoostmanesh: Data collection, Sample analysis, Writing - original draft and data interpretation.

Hossein Ahmadzadeh: Conceptualization, Data analysis, Funding acquisition, Project Supervision and data validation.

Ida Attari Navab: Data collection, Sample analysis, Review & editing.

Elham Zaeif Khorasani: Data analysis, Sample analysis.

Maryam Ijadi Bajestani: Data analysis, Review & editing.

Acknowledgement

The authors acknowledge Ferdowsi University of Mashhad for supporting this project and Dr. Mojtaba Sankian from Bu Ali Research Institute for his help in this study.

References

1. Zhang C, Zheng W, Huang X, Bell EW, Zhou X, et al. Protein Structure and Sequence Reanalysis of 2019-nCoV Genome Refutes Snakes as Its Intermediate Host and the Unique Similarity between Its Spike Protein Insertions and HIV-1. J Proteome Res. 2020; 19: 1351-1360.
2. Chung Y-S, Lee N-J, Woo SH, Kim J-M, Kim HM, et al. Validation of real-time RT-PCR for detection of SARS-CoV-2 in the early stages of the COVID-19 outbreak in the Republic of Korea. Sci Rep. 2021; 11: 14817-14824.
3. Sawano M, Takeshita K, Ohno H, Oka H. RT-PCR diagnosis of COVID-19 from exhaled breath condensate: a clinical study. J Breath Res.2021; 15: 037103-037114.
4. Gomes JC, Masood AI, Silva LH de S, da Cruz Ferreira JRB, Freire Júnior AA, et al. Covid-19 diagnosis by combining RT-PCR and pseudo-convolutional machines to characterize virus sequences. Sci Rep. 2021; 11: 11545-11572.
5. Bahadır EB, Sezgintürk MK. Lateral flow assays: Principles, designs and labels. TrAC Trends Anal Chem 2016; 82: 286-306.
6. Wu J-L, Tseng W-P, Lin C-H, Lee T-F, Chung M-Y, et al. Four point-of-care lateral flow immunoassays for diagnosis of COVID-19 and for assessing dynamics of antibody responses to SARS-CoV-2. J Infect. 2020; 81: 435-442.
7. G. Andryukov B. Six decades of lateral flow immunoassay: from determining metabolic markers to diagnosing COVID-19. AIMS Microbiol. 2020; 6: 280-304.
8. Hsiao WW-W, Le T-N, Pham DM, Ko H-H, Chang H-C, et al. Recent Advances in Novel Lateral Flow Technologies for Detection of COVID-19. Biosensors. 2021; 11: 295-320.
9. Liu H, Dai E, Xiao R, Zhou Z, Zhang M, et al. Development of a SERS-based lateral flow immunoassay for rapid and ultra-sensitive detection of anti-SARS-CoV-2 IgM/IgG in clinical samples. Sensors Actuators B Chem. 2021; 329: 129196.
10. Wen T, Huang C, Shi F-J, Zeng X-Y, Lu T, et al. Development of a lateral flow immunoassay strip for rapid detection of IgG antibody against SARS-CoV-2 virus. Analyst 2020; 145: 5345-5352.
11. Salminen T, Juntunen E, Talha SM, Pettersson K. High-sensitivity lateral flow immunoassay with a fluorescent lanthanide nanoparticle label. J Immunol Methods. 2019; 465: 39-44.
12. Wang J, Meng H-M, Chen J, Liu J, Zhang L, et al. Quantum Dot-Based Lateral Flow Test Strips for Highly Sensitive Detection of the Tetanus Antibody. ACS Omega. 2019; 4: 6789-6795.
13. Wang C, Yang X, Gu B, Liu H, Zhou Z, et al. Sensitive and Simultaneous Detection of SARS-CoV-2-Specific IgM/IgG Using Lateral Flow Immunoassay Based on Dual-Mode Quantum Dot Nano-

beads. Anal Chem. 2020; 92: 15542-15549.

14. Kim SK, Sung H, Hwang SH, Kim MN. A New Quantum Dot-Based Lateral Flow Immunoassay for the Rapid Detection of Influenza Viruses. Biochip J. 2022; 16: 175-182.

15. Oh H-K, Kim K, Park J, Im H, Maher S, Kim M-G. Plasmon color-preserved gold nanoparticle clusters for high sensitivity detection of SARS-CoV-2 based on lateral flow immunoassay. Biosens Bioelectron. 2022; 205: 114094.

16. Bai T, Wang L, Wang M, Zhu Y, Li W, Guo Z, et al. Strategic synthesis of trimetallic Au@Ag–Pt nanorattles for ultrasensitive colorimetric detection in lateral flow immunoassay. Biosens Bioelectron. 2022; 208: 114218.

17. Panraksa Y, Apilux A, Jampasa S, Puthong S, Henry CS, et al. A facile one-step gold nanoparticles enhancement based on sequential patterned lateral flow immunoassay device for C-reactive protein detection. Sensors Actuators, B Chem. 2021; 329: 129241.

18. Wang Y, Jiao W, Wang Y, Wang Y, Shen C, et al. Graphene oxide and self-avoiding molecular recognition systems-assisted recombinase polymerase amplification coupled with lateral flow bioassay for nucleic acid detection. Microchim Acta. 2020; 187: 667.

19. Khlebtsov BN, Tumskiy RS, Burov AM, Pylaev TE, Khlebtsov NG. Quantifying the Numbers of Gold Nanoparticles in the Test Zone of Lateral Flow Immunoassay Strips. ACS Appl Nano Mater. 2019; 2: 5020-5028.

20. Huang C, Wen T, Shi F-J, Zeng X-Y, Jiao Y-J. Rapid Detection of IgM Antibodies against the SARS-CoV-2 Virus via Colloidal Gold Nanoparticle-Based Lateral-Flow Assay. ACS Omega. 2020; 5: 12550-12556.

21. Yu L, Li P, Ding X, Zhang Q. Graphene oxide and carboxylated graphene oxide: Viable two-dimensional nanolabels for lateral flow immunoassays. Talanta. 2017; 165: 167-175.

22. Schubert U, Hüsing N, Laine R. Materials Syntheses. Vienna: Springer Vienna; 2008.

23. Fenger R, Fertitta E, Kirmse H, Thünemann AF, Rademann K. Size dependent catalysis with CTAB-stabilized gold nanoparticles. Phys Chem Chem Phys. 2012; 14: 9343.

24. Davardoostmanesh M, Ahmadzadeh H. A Mechanically Flexible Superhydrophobic Rock Wool Modified with Reduced Graphene Oxide-Chloroperene Rubber for Oil-Spill Clean-Up. Glob Challenges. 2021; 5: 2100072.

25. Davardoostmanesh M, Goharshadi EK, Ahmadzadeh H. Electrophoretic size fractionation of graphene oxide nanosheets. New J Chem. 2019; 43: 5047-5054.

26. https://www.imagemet.com/products_/spip/2020.

27. Zhang W, Duan H, Chen R, Ma T, Zeng L, et al. Effect of different-sized gold nanoflowers on the detection performance of immunochromatographic assay for human chorionic gonadotropin detection. Talanta. 2019; 194: 604-610.